Accepted Manuscript

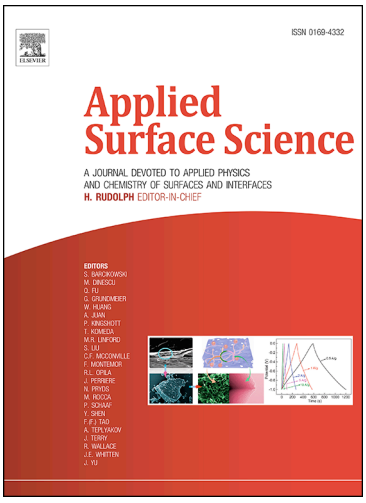

Full Length Article

Nanoscale etching of III-V semiconductors in acidic hydrogen peroxide solution: GaAs and InP, a striking contrast in surface chemistry

Dennis H. van Dorp, Sophia Arnauts, Mikko Laitinen, Timo Sajavaara, Johan Meersschaut, Thierry Conard, John J. Kelly

PII: S0169-4332(18)32606-0
DOI: https://doi.org/10.1016/j.apsusc.2018.09.181
Reference: APSUSC 40485

To appear in: *Applied Surface Science*

Received Date: 13 March 2018
Revised Date: 20 September 2018
Accepted Date: 22 September 2018

Please cite this article as: D.H. van Dorp, S. Arnauts, M. Laitinen, T. Sajavaara, J. Meersschaut, T. Conard, J.J. Kelly, Nanoscale etching of III-V semiconductors in acidic hydrogen peroxide solution: GaAs and InP, a striking contrast in surface chemistry, *Applied Surface Science* (2018), doi: https://doi.org/10.1016/j.apsusc.2018.09.181

Nanoscale etching of III-V semiconductors in acidic hydrogen peroxide solution: GaAs and InP, a striking contrast in surface chemistry

Dennis H. van Dorp[†*], Sophia Arnauts[†], Mikko Laitinen[ϕ] Timo Sajavaara[ϕ], Johan Meersschaut[†], Thierry Conard[†] and John J. Kelly[∂]

[†]Imec, Kapeldreef 75, B-3001 Leuven, Belgium

[ϕ]Department of Physics, University of Jyväskylä, P.O. Box 35, 40014, Finland

[∂]Condensed Matter and Interfaces, Debye Institute for NanoMaterials Science, Utrecht University, Princetonplein 1, 3584 CC Utrecht, The Netherlands

Corresponding Author:

*email: Dennis.vanDorp@imec.be

Abstract

In this study of nanoscale etching for state-of-the-art device technology, the importance of surface chemistry, in particular the nature of the surface oxide, is demonstrated for two III-V materials. Striking differences in etching kinetics were found for GaAs and InP in sulphuric and hydrochloric acidic solutions containing hydrogen peroxide. Under similar conditions, etching of GaAs was much faster, while the dependence of the etch rate on pH, and on H_2O_2 and acid concentrations also differed markedly for the two semiconductors. Surface analysis techniques provided information on the product layer present after etching: strongly non-stoichiometric porous (hydr)oxides on GaAs and a thin stoichiometric oxide that forms a blocking layer on InP. Reaction schemes are provided that allow one to understand the results, in particular the marked difference in etch rate and the contrasting role of chloride in the dissolution of the two semiconductors. A critical factor in determining the surface chemistry is considered to be the ease with which a proton can be removed from the group V hydroxide, which is formed in the initial etching step (the breaking of the III-V surface bond).

Keywords: nanoscale etching, GaAs, InP, reaction mechanisms, surface chemistry, III-V oxide

1. INTRODUCTION

There has recently been an upsurge of interest in III-V compound semiconductors as a result of exciting developments in device technology. These include improved fabrication techniques for flexible electronic devices,[1,2] and epitaxial integration of various III-V channel materials on Si-based platform wafers enabling the development of extremely scaled CMOS transistor technologies.[3–7] While fabrication strategies for traditional III-V optoelectronic devices such as light-emitting diodes, lasers and solar cells are well established,[8] the very small dimensions of these new nanodevices pose new problems. In such applications wet-chemical etching remains an essential step. The ever decreasing size of III-V devices requires ultimately atomic-layer-scale control of surfaces in terms of etching selectivity, stoichiometry and morphology.[9,10] Furthermore, numerous studies indicate that wet-chemical surface preparation is the key to electronic interface passivation.[11–14] There is already a considerable expertise and literature available on III-V semiconductor etching.[15–17] However, much of earlier work is empirical, etch rates are high, and insight into the underlying surface chemistry and mechanisms is often lacking.

In this work we describe the etching of GaAs and InP in acidic solutions of hydrogen peroxide (H_2O_2) in the (very) low etch rate range. H_2O_2 has been widely used as oxidizing agent for chemical etching of these semiconductors at high dissolution rate.[18–23] Potential-dependent etch rate measurements on p-type electrodes have revealed that dissolution of both semiconductors follows a purely chemical mechanism: hole injection at open-circuit potential (i.e. electroless etching) can be disregarded.[24–27] These studies showed that the etch rate of GaAs is markedly higher than that of InP.[15,26,28] The same holds for an electroless etchant such as Ce^{4+} in H_2SO_4 solution; the very low etch rate of InP was attributed to the presence of surface oxide.[15,29,30]

Our present results for the nanoscale etching range show the same trend. Under similar conditions the etch rate of GaAs in H_2SO_4/H_2O_2 solution is more than an order of magnitude higher than that of InP. (A similar high etch rate was also observed for InGaAs and InAs.[31,32]) The reason for the large difference between GaAs and InP is of fundamental interest and technological importance; the underlying chemistry has, to date, not been elucidated. A second striking result in the present study is the influence of the acid, H_2SO_4 and HCl, on etching kinetics. An increase in HCl concentration leads to an increase in the etch rate of InP while the dissolution rate of GaAs is markedly decreased (the latter is not observed in a H_2SO_4 based etchant).

This paper describes an attempt at understanding these striking differences and providing a mechanistic explanation for the contrasting behaviour of the two materials. Inductively coupled plasma mass spectrometry (ICP-MS) was used to determine the etching kinetics. Previous work suggested that the surface oxide or hydroxide may be important.[31,32] We have used X-ray photoemission spectroscopy (XPS) and time-of-flight elastic recoil detection analysis (ToF-ERDA) to obtain information about (hydr)oxide formation on the etched surfaces. XPS and ToF-ERDA measurements also allowed us the detect surface chlorine in the case of HCl-based etchants. The results indicate that, while the initial step (the breaking of the III-V surface bond) is the same for both semiconductors, the ease with which the resulting group V hydroxide entity at the surface can be deprotonated determines whether the etch rate will be high (GaAs) or low (InP). The mechanism can also help to explain the contrasting role of HCl in the dissolution of the two semiconductors.

2. EXPERIMENTAL SECTION

GaAs and InP (2 inch) substrates were obtained from AXT Inc. and Vital-Chem. The n-type wafers had a (100) orientation and a carrier concentration in the range of 5-50E+16 cm^{-3}. Chemicals were purchased from Sigma Aldrich and were of p.a. quality: 37% HCl (12.0 M), 96% H_2SO_4 (18.0 M) and H_2O_2 (9.7 M). Prior to first use, wafers were cleaned in 1 M HCl/0.25 M H_2O_2 (InP) and 0.01 M HCl/0.005 M H_2O_2 (GaAs) for 5 minutes. Before etching, the GaAs wafers were pretreated for 10 minutes in 6 M HCl and subsequently rinsed for 10 seconds in ultra-pure water (UPW) containing ~50 ppb of dissolved O_2. For InP, a 2 M HCl solution was used with an immersion time of 5 minutes.

Etching experiments were performed at room temperature in a clean room environment in a Polytetrafluoroethylene (PTFE) cell equipped with a Kalrez O-ring to expose selectively 13.85 cm^2 of the semiconductor surface to 100 mL of freshly prepared etching solution for 5-10 minutes. The solution was not stirred. Etch rate calculations are based on the total amount of dissolved ^{69}Ga, ^{75}As, and ^{115}In in the etchant solution analyzed by ICP-MS (Agilent 7500cs). Each sample was diluted and adjusted to the measurement matrix. Measurement error was determined to be within 5% and the detection limit is ~0.01 monolayer of etched III-V material. For more details we refer to previous work.[33]

Surface morphology after etching was studied with AFM using a Nanoscope Iva Dimension 3100 in tapping mode.

Surface composition was studied by angle-integrated XPS. After etching, samples were rinsed for 10 seconds in ultra-pure water containing ~50 ppb of dissolved O2. After N2 blow-drying, the samples were transported in an N2 atmosphere to the XPS set-up. The total “air exposure” was kept to ~10 minutes. The measurements were carried out in Angle Resolved mode using a Theta300 system from Thermo Instruments. 16 spectra were recorded at exit angles between 22 and 78 degrees, as measured from the normal of the sample. A monochromatized Al Kα X-ray source (1486.6 eV) was used with a spot size of 400 microns. The XPS core level spectra were fitted with Avantage software using Smart

background correction, the same relative constraints for elements and oxides and fixed FWHM fitting parameters were used. Standard sensitivity factors were used to convert peak areas to atomic concentrations. Oxide thickness was based on a model assuming a homogeneous mixed oxide layer on a III-V substrate (i.e. no variation of the Ga/As ratio with depth in the oxide). Areal density is calculated by converting the layer thickness in atoms/cm^2 assuming a bulk density of the oxide. In the case of a mixed oxide, the composition of the oxide is taken into account by using a weighted density according to its composition. Cl coverage on the substrate surface, n_x (at/cm^2) was calculated by the formula:

$$n_x = \frac{I_x}{I_{Sub}} * l_{Sub} * N_{Sub}$$

where I_x and I_{sub} are the the peak intensities of the species and substrate, respectively, l_{Sub} is the effective attenuation length for quantitative analysis (NIST data base) and N_{Sub} is the atomic concentration (Ga+As) in the substrate (at/cm^3).[34]

Time-of-flight elastic recoil detection analysis (ToF-ERDA) was used for O and Cl quantification. After etching, samples were N_2 blow-dried and transported and loaded within ~5 minutes in the experimental setup vacuum. Oxygen was measured at Imec using an 8 MeV $^{35}Cl^{4+}$ ion beam.[35] The incidence angle of the beam was 20° from grazing incidence. The signal from recoil oxygen is well separated in the spectrum and easily measured. The integrated signal from oxygen for the present samples was around 30 counts. The signal from ^{35}Cl ions scattered on the heavy element (In or Ga) was used to determine the ion fluence. Elemental Cl surface concentrations were measured using a 13.6 MeV $^{127}I^{7+}$ incident ion beam from the 1.7 MV Pelletron accelerator at the Accelerator Laboratory of the University of the Jyväskylä.[36,37] While the detector scattering angle was 41°, the sample was tilted so that its surface was at an angle of 33.5° to the beam direction and 7.5° to the detectors. Elemental Cl concentration was calculated from the recoil yield with the assumption that all detected Cl

atoms are coming from the surface. In these measurements with heavy incident ions and substrate atoms, the uncertainty of the beam fluence and therefore also the final concentration is estimated to be about 20 %. The elemental losses due to the ion beam bombardment were analyzed in the Potku software and corrected to provide the original concentration at the beginning of the measurement.[38]

3. RESULTS

3.1 Etching kinetics: a comparison of GaAs and InP

Etching results for the two semiconductors are presented in Figure 1. In order to achieve nanoscale etching for GaAs it was essential to use a low concentration of the oxidizing agent in the etchant. This was not the case for InP.

GaAs (100). After the cleaning step (see Experimental) and prior to etching, the GaAs wafers were pretreated in a 6M acid solution to remove the native oxide. The wafers were subsequently shortly rinsed with UPW before etching. The etch rate of GaAs in 1 M H_2SO_4 solution containing H_2O_2 increases linearly with increasing concentration of the oxidizing agent in the range 0-0.05 M (Figure 1(a)). A linear dependence is also found for a 1 M HCl solution, although the etch rate in this range is considerably lower than for the H_2SO_4 etchant. Figure 1(b) gives the etch rate of GaAs as a function of proton concentration at constant H_2O_2 concentration (0.02 M). In both acids the etch rate is low at low H^+ concentration (< 0.001 M) and increases with increasing acidity (up to 0.01 M H^+). In the case of H_2SO_4 the etch rate levels off from 0.01 M H^+, remaining essentially constant up to 1 M. In this range it has been shown that etching is kinetically controlled, i.e. mass transport is not important.[24] In

contrast, for HCl the etch rate passes through a maximum at about 0.01 M and decreases markedly as the HCl concentration is raised to 1 M. This decrease continues up to 6 M HCl at which the etch rate is 0.5 nm min^{-1} (not shown in the figure). A similar difference between etchants based on H_2SO_4 and HCl has also been observed for InGaAs[31] and InAs.[32]

InP (100). The kinetics of etching of InP differs in a number of respects from that described above for GaAs. The etch rate, like that of GaAs, increases with increasing H_2O_2 concentration for both 1 M H_2SO_4 and 1 M HCl solutions, see Figure 1(c) (note the higher H_2O_2 concentration range in this figure). However, in the case of InP the HCl etchant gives a measurably higher etch rate than the H_2SO_4 etchant above 0.2 M H_2O_2. Figure 1(d) shows that at constant H_2O_2 concentration (1 M) the InP etch rate for both etchants increases with increasing acid concentration (compare with figure 1(b)). Again, the etch rate in HCl is higher than that in H_2SO_4; the relative enhancement of the etch rate increases with increasing HCl concentration. This is also the case for more dilute H_2O_2 solutions (see reference[39]). Finally, we point out that the etch rate of InP in both acids is significantly lower than that of GaAs in solutions of similar composition. For example, in a 1 M H_2SO_4 / 0.1 M H_2O_2 solution the etch rate of InP is 0.7 nm min^{-1} while that of GaAs is 30 nm min^{-1}.

3.2 Surface Analysis

The purpose of our surface analysis with XPS was not to obtain detailed information about the chemical nature of the group III and group V products produced on the surface by etching. We were mainly interested in the product layer (oxide or hydroxide), its thickness and stoichiometry, in relation to the etching process. As will become clear, the use of a water rinsing step after pretreatment of GaAs (100) in a 6 M HCl solution or etching in HCl/H_2O_2 solutions plays an important role in determining the

surface chemistry, in particular that of surface chlorine. The results obtained with and without the water rinse are described in the following two sections. The final section is devoted to InP etched in H_2SO_4 and HCl solutions containing H_2O_2.

GaAs (100), with water rinse. The nature of the acid solution and its pH are important in determining the etching kinetics of GaAs in the present study (see Figure 1(b)). To obtain insight into dissolution mechanisms the etched surface was studied ex-situ by XPS and ToF-ERDA. Results were obtained for HCl and H_2SO_4 etchants with 0.01M H_2O_2 and three acid concentrations: 1.0 M, 0.01 M and 0.001 M, each corresponding to distinctive etching characteristics.

As for the etching experiments, GaAs was pretreated in 6 M HCl solution and subsequently rinsed with UPW. This served as a reference in the case of HCl etchants. (The etch rate of GaAs in this medium is very low, ~0.5 Å min^{-1}.[32]) Figure 2 gives angle-integrated XPS spectra: (a) for As 3d and (b) for Ga 3d. The corresponding deconvoluted spectra show contributions from As $3d_{3/2}$, As $3d_{5/2}$ and As(III)-O (Figure 2(a)) and Ga $3d_{3/2}$, Ga $3d_{5/2}$ and Ga(III)-O (Figure 2(b)). The As(III)-O and the Ga(III)-O can be attributed to oxide or hydroxide. In this work we cannot distinguish between these two possibilities. The areal density of oxide on the surface is 8E+14cm^{-2}. The presence of oxygen was confirmed by ToF-ERDA measurements that showed an areal density of 1E+15 cm^{-2}. Clearly, the surface layer is As-rich; the As-O/Ga-O ratio was 7. In order to obtain an indication of trends in layer thickness, we consider a mixed oxide as product layer. The layer thickness estimated from these XPS measurements was 0.3 nm. According to various authors GaAs (100), pretreated in HCl solution, should be essentially oxide-free.[40–44] Oxide growth, observed with our sample, must have occurred during the water rinsing step and/or transfer of the sample to the spectrometer; the conditions were not completely oxygen-free.

Figure 3 shows angle-integrated XPS spectra for GaAs etched in 0.01 M H_2O_2 solution with 3 different HCl concentrations (1 M, 0.01 M and 0.001 M). In the case of 1 M HCl (Figure 3(a), (b)) the measured spectra and the deconvoluted peaks are very similar to those of the reference sample (Figure 2): d_{ox} = 0.4 nm, areal density = 1E+15 cm^{-2}, As-O/Ga-O = 5. This could mean that the oxide detected after etching is, as in the 6 M HCl case, due to oxide regrowth. Alternatively, the oxide could have resulted from etching. The measurements do not allow us to decide in this case. For the 0.01 M HCl etchant (Figure 3(c), (d)) the general features of the (deconvoluted) spectra are the same as for the 1 M solution. However, the As(III)-O and Ga(III)-O peaks are stronger, indicating a higher oxide coverage on the surface. The corresponding layer thickness is 0.7 nm (areal density = 2E+15 cm^{-2}).

Three new features are obvious in the spectra for 0.001 M HCl solution. The As(III)-O and Ga(III)-O peaks are now dominant, indicating a significantly thicker (hydr)oxide than that formed in the 0.01 M HCl case: 4.1 nm (areal density = 2E+16 cm^{-2}) versus 0.7 nm (the corresponding value for the 1 M etchant was 0.4 nm, see above). This difference is supported by the ToF-ERDA measurements which gave oxygen areal densities of 3E+16 cm^{-2} and 4E+15 cm^{-2} for 0.001 and 0.01 M HCl, respectively (Figure 4). A striking result in this case is the As-O/Ga-O ratio; 20 for 0.01 M HCl; 0.3 for 0.001 M HCl. Clearly, the (hydr)oxide layer is As-rich at higher proton concentration, Ga-rich at lower concentration. Finally, in the 0.001 M HCl case, there is a measurable contribution from As(V)-O to the (hydr)oxide peak (Figure 3(e)).

There are strong similarities between the XPS results observed with HCl and H_2SO_4 (compare Figures 2 and 3 with Figures S1 and S2 (see Supplement), respectively. After pretreatment in 6 M H_2SO_4, an As(III)-O peak and a weaker Ga(III)-O peak are also found. The layer thickness in this case is the same as that for 6 M HCl (0.3 nm). Etching in 1 M H_2SO_4/0.01 M H_2O_2 solution leads to an increase in the As(III)-O peak and layer thickness (0.4 nm). The Ga(III)-O contribution is, in this case, also weaker than that of As(III)-O, i.e. the oxide is As-rich. The 0.001 M H_2SO_4 etchant gave a much thicker

surface layer (4.2 nm) than the 0.01 M acid solution (0.5 nm). This difference was also supported by ToF-ERDA measurements (3E+16 cm^{-2} and 2E+15 cm^{-2} for 0.001 M and 0.01 M, respectively). As in the HCl case, the layer formed in the 0.01 M H_2SO_4 solution was As-rich (As-O/Ga-O = 11) while that formed in the 0.001 M solution was Ga-rich (As-O/Ga-O = 0.2). As in the HCl case, a measurable contribution is observed from As(V)-O for the 0.001 M H_2SO_4 solution.

GaAs (100), without water rinse. From Figure 1 the importance of the chloride concentration on etching is clear: the etch rate decreases markedly as the HCl concentration is increased from 0.01 to 1.0 M. Chlorination of GaAs surfaces has been observed for HCl solution in the absence of a strong oxidizing agent.[45–48] From the literature there is evidence that suggests that a water rinse between emersion of the wafer and the XPS measurement may be critical.[49] For this reason we performed a series of etching experiments to investigate the effect of omitting the water rinsing step on the resulting XPS spectra, including the Cl features. Figure 5 shows spectral features for As 3d and Ga 3d measured after etching the GaAs sample in 1 M HCl / 0.01 M H_2O_2. Two differences are observed as compared to the rinsed sample (Figure 3 (a,b)). First, the high binding energy component for the As 3d peak is smaller, indicating that water rinsing results in some reoxidation. Second, a significantly larger contribution of comparable chemical shift is observed in the case of Ga 3d. Two distinct spin-orbit split peaks in the Cl 2p spectrum ($p_{3/2}$ and $p_{1/2}$) shows that Ga(III)-Cl is very likely important (Figure 5(c)). However, the presence of Ga(III)-O cannot be excluded due to a similar expected chemical shift.[43] Based on spectral component analysis a chloride coverage of 6E+14 cm^{-2} was calculated. (No Cl was measured by XPS when the etched sample had been water-rinsed.) Our ToF-ERDA measurements (Figure 5(d)) confirm the presence of Cl on GaAs etched in HCl solution containing H_2O_2, when the sample was not water-rinsed. A Cl areal density of 6E+14 cm^{-2} was detected after etching for 10 minutes in 1 M HCl / 0.01M H_2O_2 solution. In contrast, the Ga 3d features for the unrinsed sample etched in 0.01 M HCl /

0.01 M H_2O_2 solution were comparable to those of the rinsed sample (not shown). Figure 5(c) shows that the surface Cl concentration was low (8E+13 cm^{-2}).

For the reference sample, pretreated in 6 M HCl but not rinsed, an increase in the higher binding energy component of the Ga 3d peak was also observed. The Cl concentration was high (5E+14 cm^{-2}), a value comparable to the 1 M HCl / 0.01 M H_2O_2 etched samples. The Cl concentration of the rinsed 6 M HCl sample was markedly lower (4E+13 cm^{-2}).

InP(100). Angle-integrated XPS spectra for P 2p and In 3d are shown for HCl etchants in Figure 6 and for H_2SO_4 etchant in Figure S3 of the supplement. The P 2p spectra show contributions from P $2p_{1/2}$, P $2p_{3/2}$ and P(III)-O. Although the In $3d_{5/2}$ peak is more difficult to fit due to the small chemical shift of In(III)–O with respect to the In–P bulk contribution, the summed intensities of the spectra provide more confidence in the fitting parameters. The lower HCl concentration (2 M) used for the reference sample (Figure 5(a), (b)), was chosen to avoid the risk of chemical etching of InP by HCl.[15] A very small contribution from In(III)-O and P(III)-O indicates, in contrast to GaAs, a very low oxide coverage on the surface (see also reference [50]). The same holds for the H_2SO_4 pretreatment. Here, the experimental procedure was the same as that used for GaAs, with possible exposure of the sample to oxygen during the water rinse and sample transfer to the XPS spectrometer. The surface of InP etched in acidic 1 M H_2O_2 solutions was different in two important respects from that of GaAs. First, the oxide on InP is very thin (~0.2 nm, areal density = 8E+14cm^{-2}) for both HCl and H_2SO_4 etchants. ToF-ERDA measurements performed on such etched samples showed a very low oxygen areal density (1E+15 cm^{-2}). In addition, XPS shows that the oxide has an P-O/In-O stoichiometry in the range 0.8 – 1, in strong contrast to that of GaAs.

4. DISCUSSION

4.1 Etching mechanisms: a comparison of GaAs and InP

Using the information obtained from XPS and ToF-ERDA we propose general reaction schemes for the dissolution of GaAs and InP. To support the conclusions with respect to the influence of chloride in the case of GaAs, surface roughness produced by etching, was checked by AFM for HCl concentrations up to 6 M. Finally, we consider the origin of the marked differences in etching properties of the two semiconductors.

GaAs (100)/H_2SO_4. From Figure 1, it is clear that there are two distinct regimes for etching of GaAs in dilute H_2O_2 solutions. These are defined by the relative acid content of the acid. At higher H^+ concentration ($\geq$ 0.01 M for 0.02 M H_2O_2) the etch rate is independent of pH. At lower proton concentration, the etch rate decreases with increasing pH to a very low value below 0.001 M. The (hydr)oxide present on the etched surface differs markedly for the two ranges: a relatively thin layer (0.3-0.7 nm) that is As-rich for the "active" etching range ($\geq$ 0.01 M H^+); a thick layer (4.1-4.2 nm), Ga-rich at high pH (0.001 M H^+). Since, in the active range, the etch rate is constant for a given etchant composition and is linearly dependent on the H_2O_2 concentration, we conclude that the surface (hydr)oxide layer does not hinder dissolution, i.e. it must be porous. The formation of a Ga-rich layer at high pH lowers the etch rate, finally suppressing etching completely below 0.001 M H^+. The strong non-stoichiometry of the oxide in both ranges indicates that a coherent mixed Ga/As oxide does not play an essential role in etching of GaAs under the present conditions.

To explain the results in the active etching range, we suggest a simplified scheme consisting of two equivalent paths (Reaction Scheme 1). Photoelectrochemical experiments [24,25] have provided evidence to show that the first step in chemical etching involves a synchronous exchange of bonds between HO-OH and Ga-As surface bonds, as first proposed by Gerischer and Mindt.[27] Two steps are involved, shown schematically in reactions 1(a) and 1(b). Transfer of a bonding electron from a GaAs surface bond to an H_2O_2 molecule at the surface produces a new As-OH bond, an $OH^{\bullet}$ radical and an electron-deficient bond (reaction 1(a)). The highly reactive $OH^{\bullet}$ radical immediately extracts the second electron from the bond, giving rise to a polar Ga-OH bond (reaction 1(b)).

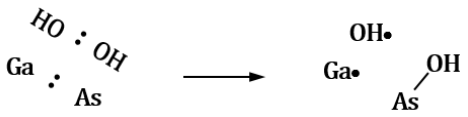

1(a)

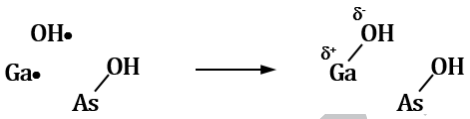

1(b)

The primary product for both surface atoms is a hydroxide (this may subsequently undergo conversion to oxide). If the proton concentration is high (> 0.01 M), the Ga-OH bond will be hydrolyzed (blue path, step 2A in Reaction Scheme 1). This gives a surface Ga^{+} whose charge is balanced by the acid anion in the solution double layer (shown as A^{-} in the reaction scheme). When this sequence is twice repeated Ga^{3+} and $As(OH)_3$ are formed as products (step 3A). Reaction step 1 is rate-determining. $As(OH)_3$,

arsenous acid, is a very weak acid and will not dissociate under these conditions.[51] Since an As-rich product layer is detected, we include a second step (4A), parallel to step 3A, in which $As(OH)_3$ builds up at the surface. To simplify the scheme we omit the contribution of Ga hydroxide that constitutes only a small fraction of the total layer in this pH range (see below). The layer thickness will be determined by the rate of deposition of $As(OH)_3$ on the surface and its dissolution.

In principle, As(III) can be oxidized to As(V) by H_2O_2.[52,53] In the case of $As(OH)_3$ this will lead to the formation of the strong arsenic acid ($O=As(OH)_3$). However, in solution this reaction is reported to be slow unless $OH^{\bullet}$ radicals are produced by a Fenton-type reaction.[54] That As(V) is unlikely to be formed by direct etching is supported by the results of anodic etching of p-type GaAs and photoanodic etching of n-type GaAs in acidic solution. In both cases six charge carriers are required to dissolve one formula unit of GaAs indicating trivalent products. Our XPS results, however, reveal the presence of an As(V) component in the product layer formed in 0.001 M acid solutions (see Figure 3 and supplement). It has been reported that the rate of oxidation of As(III) can be promoted by surface catalysis when adsorbed on a solid substrate, e.g. alumina and non-ferrous metal oxides. [55,56] We speculate that Ga (hydr)oxide, formed on the surface at this pH, may act as a catalyst for As(III) oxidation.

In Reaction Scheme 1, dissolution of GaAs in the active etching range proceeds via two parallel paths: directly (3A) and indirectly via hydroxide formation and dissolution (4A). While the latter obviously must occur, we propose that it accounts for only a fraction of the total etching result. There is no obvious relationship between the surface layer thickness and the etch rate for either the H_2SO_4 or the HCl etchant. The XPS and ERDA measurements show that in both cases the layer thickness is higher for the 0.01 M acid solution than for the 1 M solution. In this pH range the etch rate for the H_2SO_4 solution is constant while that in HCl is markedly higher for the case of the thicker surface layer (at 0.01 M HCl). An exclusive surface layer formation / dissolution mechanism would lead to quite different kinetics (see InP/H_2SO_4, HCl section below).

At higher pH, the low proton concentration has two effects: first, the rate of hydrolyzation of surface Ga-OH (step 2A) is decreased significantly so that $Ga(OH)_3$, or an equivalent (sub-)oxide, can be deposited on the surface (red path, step 2B); second, the rate of dissolution of such a (hydr)oxide (step 3B) decreases with decreasing proton concentration. It is therefore not surprizing that a thick Ga-rich surface layer is formed for $[H^+] < 0.01$ M resulting in a 4 nm layer at 0.001 M H_2SO_4. It is also not surprizing that such a layer finally prevents dissolution of the semiconductor, as shown in Figure 1. In this range (<0.01 M H^+), $As(OH)_3$ continues to be formed. Although the surface layer is Ga-rich, the As product constitutes 20% of the layer for an etchant of pH 3.

GaAs (100)/HCl. As in H_2SO_4, the etch rate of GaAs in HCl solution (0.02 M H_2O_2) drops as the proton concentration decreases below 0.01 M (Figure 1). The 0.001 M HCl etchant, as in the H_2SO_4 case, gives rise to a thick Ga-rich oxide and the etch rate is low. Surprizingly, the etch rate shows a maximum at about 0.01 M HCl (the decrease continues up to 6 M HCl). This trend was also observed with InGaAs[31] and InAs[32] in H_2O_2/HCl etchants.

There is a considerable literature showing that pretreatment of GaAs in aqueous HCl solution leads to chlorine adsorption on the surface. XPS measurements on GaAs (111)A revealed the presence of an ordered monolayer of Cl.[42,45,48] That this layer removes bandgap surface states caused by surface oxides was confirmed by photoluminescence and photovoltage experiments.[42,48] The chlorinated surface was reported to be stable in air.[48] Chlorine adsorption at high coverage on GaAs (100) surfaces has also been observed by XPS after etching in HCl solution.[40–42] Our XPS measurements confirm that pretreatment of GaAs (100) in 6 M HCl gives rise to a high areal density of Cl on the surface, provided the wafer is not rinsed with water prior to surface analysis. We found, in addition, that etching of GaAs (100) in a 1 M HCl solution containing a strong oxidizing agent (0.01 M H_2O_2) gives

rise to the formation of approximately a monolayer of Cl on the surface, that can be detected by XPS and ToF-ERDA, again in the absence of a water rinse (see section 3.2). The Cl coverage after etching in a more dilute HCl solution (0.01 M HCl/0.01M H_2O_2) was markedly lower.

The chloride ion is a complexing agent for the Ga^{3+} cation. As such, it can be expected to influence Reaction scheme 1 by reacting with Ga^+ or Ga-OH at the surface to give a Ga-Cl surface entity.

$$Ga_s^+ + HCl \rightarrow Ga\text{-}Cl_s + H^+ \qquad 2(a)$$

$$Ga\text{-}OH_s + HCl \rightarrow Ga\text{-}Cl_s + H_2O \qquad 2(b)$$

That such reactions occur during etching of GaAs (100) in 1M HCl/0.01M H_2O_2 solution is supported by the change observed in the Ga 3d peak at binding energy of approximately 21 eV when the water rinsing step is avoided and a high Cl surface coverage is detected. (In the literature described above, Cl is reported to form a perfect monolayer on the (111)-A surface of GaAs pretreated in concentrated HCl. [45,48]) Equations 2(a) and 2(b) indicate that the Ga product will be a complex of the form $GaCl_n^{(3-n)+}$, where $1 \leq n \leq 3$. The value of n depends on how efficiently the reactions corresponding to equations 2(a) and 2(b) compete with step 2A/3A/4A and 2B/3B of Reaction Scheme 1. This will depend on the HCl concentration. For example, in the case of n=2 the total reaction will take the form

$$GaAs + 3H_2O_2 + 3HCl \rightarrow GaCl_2^+ + As(OH)_3 + 3H_2O + Cl^- \qquad (2c)$$

The final product in solution will be a Ga-chloro/aquo complex. At low HCl concentration, formation of $Ga(OH)_3$ is favoured, rather than Ga chlorination (equations 2(a-c)) and, as in the H_2SO_4 case, a thick Ga-rich product layer is formed.

Reaction 2(b) suggests a reason for the importance of the rinsing step between emersion of the GaAs wafer and surface analysis. If this reaction is to some extent reversible, then exposure of a chlorinated surface to water will remove the chlorine from the surface and oxide regrowth will occur. Oxidation of the GaAs surface by oxygen present, even at a low concentration, in UPW may contribute to removal of Cl from the surface during rinsing. We cannot rule out the possibility that Cl also bonds to As at the surface. However, the As-Cl bond is expected to be considerably less stable in water than the Ga-Cl bond ($AsCl_3$ hydrolyzes readily in water and moist air).

Considering the stability of Cl-terminated GaAs in air, mentioned above, it is perhaps not surprizing that surface Cl influences the dissolution kinetics of the semiconductor in the present etchants. This is likely due to steric hindrance, preventing easy access of H_2O_2 to the GaAs surface bonds. In addition, the presence of Cl at the surface may stabilize the back bonds. The clear effect of a low concentration of HCl on etch rate, e.g. 0.03 M (see Figure 1), suggests that preferential adsorption may occur initially at the more active etching sites. This leads one to expect that etching in HCl might give rise to flat surfaces. To check this hypothesis surface morphology was examined by AFM. After etching a layer of 10 nm in 1 M HCl/0.01 M H_2O_2 solution, small hillocks are visible across the full surface indicating that etching is not uniform (Figure 7a). The RMS roughness is 1.1 nm. At high HCl concentration hillock formation is suppressed. This is clear from Figure 7b, which shows the result for a pristine sample, 10 nm of which was etched in 6 M HCl/0.01 M H_2O_2. A smooth surface with an RMS roughness of 0.3 nm was obtained, a value close to that of the unetched surface (Figure 7c, RMS = 0.2 nm). A similar result has been observed for InGaAs.[31] These results support the idea that passivation of active surface

etching sites by Cl atoms reduces the overall reactivity of the surface and, with that, the surface roughness.

InP/H_2SO_4, HCl. The etch rate of InP in acidic H_2O_2 solution is markedly lower than that of GaAs for similar etchant composition. To achieve significant etching for InP, high H_2O_2 and acid concentrations are essential (see Figure 1). In contrast to GaAs at low pH, the etch rate of InP increases as both the H^+ and H_2O_2 concentrations are increased. ToF-ERDA and XPS measurements show the presence of a very thin, nearly stoichiometric oxide on InP exposed to both H_2SO_4 and HCl etchants.

From the etching results and surface analysis we conclude that in H_2SO_4/H_2O_2 solution a coherent blocking film is formed on InP. This layer must be etched to permit access of H_2O_2 to InP surface bonds and further oxidation of the semiconductor. The first step in Reaction Scheme 2 is the same as that proposed for GaAs in Reaction Scheme 1. Condensation of the resulting In-OH and P-OH groups (step 2A) leads to the formation of an In-O-P bridge and loss of H_2O. Extension of this bridge structure towards the back bonds gives rise to a stoichiometric oxide layer (step 3) which hinders dissolution of the semiconductor. The steady-state etch rate is determined by the rates of oxide formation and dissolution; the latter depends on the proton concentration (Step 4). In solution, $\{P(OH)_3\}_s$ will convert to phosphorous acid.[57] Direct dissolution, as for GaAs (Reaction Scheme 1, steps 2A/3A), is clearly not favourable in the case of InP.

As expected, the picture changes somewhat for the HCl etchant. Via step 2B of Reaction Scheme 2, In–OH can be converted to In–Cl with the loss of H_2O. This reaction prevents In–O–P bridge formation at that site and thus hinders passivation. At the same time, it would seem to open up a new parallel path to etching, giving as products $InCl_3$ and $P(OH)_3$. However, the contribution of this process is likely to be limited. In order for an $InCl_3$ entity to dissolve in solution all the back bonds to the chlorinated surface

In atom must also be chlorinated before an In–O–P bridge is formed in any one of them: the bridged oxygen anchors the chlorinated surface atom in the lattice. In this way chlorine is built into and will likely "disturb" the oxide lattice. We attribute the enhancement of the etch rate of InP in HCl solution to an increase in etch rate of the oxide caused by incorporation of Cl.

It is interesting to compare these results with those reported for InP in acidic bromine solutions.[58] Like H_2O_2, Br_2 is a chemical etchant for III-V semiconductors, including GaAs and InP. (The two oxidizing agents also share photoelectrochemical properties.[24]) Surprizingly in the context of the present work, the etch rate of InP (100) in acidic Br_2/KBr solution is much higher than that reported here for acidic H_2O_2 solution. For example, a 0.1 M Br_2 solution gives an etch rate of 600 nm/min (compare Figure 1(c)). In the case of Br_2, the initial bond-breaking step, analogous to step 1 in Reaction Scheme 2, yields In-Br and P-Br bonds that will prevent oxide formation (step 2A). In this way, an "active" surface is maintained, thus ensuring a high etch rate. This is clearly a more effective process than that involving a Cl^- reaction after the In-P surface bond has been broken by H_2O_2 (see Reaction scheme 3).

4.2 The critical step in oxide formation

The question remains as to why etching kinetics and oxide formation are so different for the two semiconductors in acidic H_2O_2 solution. An important observation is that etching of InAs in these solutions is quite similar to that of GaAs, as described in the present paper.[32] The trends in the low and high pH ranges are the same. This indicates that the formation of a blocking layer on InP is very likely not determined by In but by the group V atom at the surface. To take into account the role of P in the formation of a coherent oxide via In–O–P bridge formation we note that step 2A in Reaction Scheme 2 must be considered naive. Such a condensation reaction will not occur directly but must very likely be catalyzed by protons (step 1, Reaction Scheme 3). We propose that the oxygen bridge is caused

by electrostatic interaction between an electron lone pair on the oxygen of the P–OH and the positive charge on the indium (see inset Reaction Scheme 3). At the same time a proton is released from the OH group to solution; we consider this to be the critical step. The ease with which deprotonation takes place will be determined by the relative "acidity" of the group V hydroxide (P–OH in this case). We can get an indication of this from the acidity of the corresponding acids: phosphorous acid in the case of $P(OH)_3$ and arsenous acid $As(OH)_3$. The former is a strong acid the latter a weak acid (the pK_a values are 1.3 and 9.3, respectively).[51,57] If this trend is also valid for the P–OH and As–OH groups at the surface then it is clear why bridge formation is favoured in InP and not in GaAs. For this reason Ga–O–As bridge formation is not included in Reaction Scheme 1, step 3A and/or 2B being favoured kinetically. As the surface analysis results show a non-blocking composite (hydr)oxide is formed (step 2B) whose stoichiometry is determined by the pH of the etchant. In the case of InP the equivalent steps are unfavourable compared to oxygen-bridge formation (step 2A, Reaction Scheme 3).

SUMMARY AND CONCLUSIONS

Three main issues related to the chemical etching of III-V semiconductors in acidic hydrogen peroxide solution are addressed in this paper:

(i) the difference in kinetics of etching of GaAs in H_2SO_4 for two pH ranges: pH $\leq$ 2 and pH > 2;

(ii) the influence of Cl^- ions on etching of GaAs in the low pH range;

(iii) the radically different etching kinetics observed for InP, including the role of chloride ions.

Ex-situ surface analytical techniques (XPS, ERD) in combination with ICP-MS were used to obtain information about these systems. These show:

(i) For GaAs in H_2SO_4 etchant at low pH ≤ 2, an As-rich film ($As(OH)_3$) is present on the surface. The film doesn't interfere with etching. The etch rate is independent of pH and directly proportional to the H_2O_2 concentration. At pH > 2, the solubility of the Ga (hydr)oxide becomes a problem and a thick Ga-rich oxide is formed on the surface. This layer retards etching and is approximately 4 nm thick and passivates the surface. A reaction scheme involving two parallel routes can account for these results.

(ii) In HCl etchants in the pH range ≤ 2, the Cl^- ion decreases the etch rate of GaAs; the degree depends on the HCl concentration. XPS and ToF-ERDA shows the presence of Cl on the surface of such samples after etching. We suggest that Cl^- forms a complex with oxidized Ga at the surface. This process deactivates active etching sites, thereby reducing the etch rate. As a result, such etchants containing a high HCl concentration (e.g. 6 M) give surfaces with low surface roughness.

(iii) That the etch rate of InP is markedly lower than that of GaAs for similar etching conditions is attributed to the formation of a thin (nearly) stoichiometric blocking oxide on the surface. The rate of dissolution of this oxide determines the etch rate which increases as a function of the H_2SO_4 and H_2O_2 concentrations. In contrast to GaAs, the etch rate is enhanced by Cl^- ions. One step in the reaction scheme for InP, the formation of a In–O–P bridge, is particularly important in accounting for the results. It is suggested that easy release of a proton by the P–OH surface group (in contrast to As–OH) is responsible for oxide formation on InP and thus the marked difference in etching kinetics of the two semiconductors.

ABBREVIATIONS

AFM, atomic force microscopy; ICP-MS, inductively coupled plasma mass spectrometry; XPS, x-ray photoemission spectrometry; GaAs, gallium arsenide; InP, indium phosphide; ToF-ERDA, time of flight elastic recoil detection analysis; TXRF, total reflection x-ray fluorescence;

ACKNOWLEDGEMENTS

This work is part of the imec Industrial Affiliation Program on III-V/Ge devices. The authors acknowledge Screen Semiconductor Solutions Co. Ltd., Entegris ATMI, Kurita and Fuji Film Electronic Materials for their contributions to the Joint Development Program. We would like to thank Danielle Vanhaeren for supporting the AFM measurements and Frank Holsteyns for management support.

REFERENCES

[1] C.-W. Cheng, K.-T. Shiu, N. Li, S.-J. Han, L. Shi, D.K. Sadana, Epitaxial lift-off process for gallium arsenide substrate reuse and flexible electronics, Nat. Commun. 4 (2013) 1577. doi:10.1038/ncomms2583.

[2] N.J. Smeenk, J. Engel, P. Mulder, G.J. Bauhuis, G. Bissels, J.J. Schermer, E. Vlieg, J.J. Kelly, Arsenic formation on GaAs during etching in HF solutions: relevance for the epitaxial lift-off process, ECS J. Solid State Sci. Technol. 2 (2013) P58–P65.

[3] J.A. del Alamo, Nanometre-scale electronics with III–V compound semiconductors, Nature. 479 (2011) 317–323. doi:10.1038/nature10677.

[4] M. Paladugu, C. Merckling, R. Loo, O. Richard, H. Bender, J. Dekoster, W. Vandervorst, M. Caymax, M. Heyns, Site Selective Integration of III–V Materials on Si for Nanoscale Logic and Photonic Devices, Cryst. Growth Des. 12 (2012) 4696–4702. doi:10.1021/cg300779v.

[5] N. Waldron, C. Merckling, L. Teugels, P. Ong, S.A.U. Ibrahim, F. Sebaai, A. Pourghaderi, K. Barla, N. Collaert, A.V.-Y. Thean, InGaAs Gate-All-Around Nanowire Devices on 300mm Si Substrates, IEEE Electron Device Lett. 35 (2014) 1097–1099. doi:10.1109/LED.2014.2359579.

[6] K. Tomioka, M. Yoshimura, T. Fukui, A III-V nanowire channel on silicon for high-performance vertical transistors, Nature. 488 (2012) 189–192. doi:10.1038/nature11293.

[7] M. Heyns, W. Tsai, Ultimate scaling of CMOS logic devices with Ge and III–V materials, Mrs Bull. 34 (2009) 485–492.

[8] S.J. Pearton, C.R. Abernathy, F. Ren, Topics in Growth and Device Processing of Iii-V Semiconductors, World Scientific Pub Co Inc, Singapore; River Edge, NJ, 1996.

[9] K.J. Kanarik, T. Lill, E.A. Hudson, S. Sriraman, S. Tan, J. Marks, V. Vahedi, R.A. Gottscho, Overview of atomic layer etching in the semiconductor industry, J. Vac. Sci. Technol. Vac. Surf. Films. 33 (2015) 020802. doi:10.1116/1.4913379.

[10] G.S. Oehrlein, D. Metzler, C. Li, Atomic Layer Etching at the Tipping Point: An Overview, ECS J. Solid State Sci. Technol. 4 (2015) N5041–N5053. doi:10.1149/2.0061506jss.

[11] H. Hasegawa, M. Akazawa, Surface passivation technology for III–V semiconductor nanoelectronics, Appl. Surf. Sci. 255 (2008) 628–632. doi:10.1016/j.apsusc.2008.07.002.

[12] H. Hasegawa, M. Akazawa, Interface models and processing technologies for surface passivation and interface control in III–V semiconductor nanoelectronics, Appl. Surf. Sci. 254 (2008) 8005–8015. doi:10.1016/j.apsusc.2008.03.051.
[13] G. Brammertz, H.-C. Lin, K. Martens, D. Mercier, S. Sioncke, A. Delabie, W.E. Wang, M. Caymax, M. Meuris, M. Heyns, Capacitance-voltage characterization of GaAs–Al[sub 2]O[sub 3] interfaces, Appl. Phys. Lett. 93 (2008) 183504. doi:10.1063/1.3005172.
[14] C. Adelmann, D. Cuypers, M. Tallarida, L.N.J. Rodriguez, A. De Clercq, D. Friedrich, T. Conard, A. Delabie, J.W. Seo, J.-P. Locquet, S. De Gendt, D. Schmeisser, S. Van Elshocht, M. Caymax, Surface Chemistry and Interface Formation during the Atomic Layer Deposition of Alumina from Trimethylaluminum and Water on Indium Phosphide, Chem. Mater. 25 (2013) 1078–1091. doi:10.1021/cm304070h.
[15] P.H.L. Notten, J.E.A.M. Meerakker, J.J. Kelly, Etching of III-V semiconductors: an electrochemical approach, Elsevier Advanced Technology, 1991.
[16] A.R. Clawson, Guide to references on III–V semiconductor chemical etching, Mater. Sci. Eng. R Rep. 31 (2001) 1–438.
[17] S.J. Pearton, Wet and dry etching of compound semiconductors, Handb. Compd. Semicond. (1995) 370–441.
[18] D.W. Shaw, Localized GaAs Etching with Acidic Hydrogen Peroxide Solutions, J. Electrochem. Soc. 128 (1981) 874–880. doi:10.1149/1.2127524.
[19] J.J. Kelly, A.C. Reynders, A study of GaAs etching in alkaline H2O2 solutions, Appl. Surf. Sci. 29 (1987) 149–164. doi:10.1016/0169-4332(87)90001-8.
[20] H.K. Kuiken, J.J. Kelly, P.H.L. Notten, Etching Profiles at Resist Edges I. Mathematical Models for Diffusion-Controlled Cases, J. Electrochem. Soc. 133 (1986) 1217–1226.
[21] P.H.L. Notten, J.J. Kelly, H.K. Kuiken, Etching Profiles at Resist Edges II. Experimental Confirmation of Models Using, J. Electrochem. Soc. 133 (1986) 1226–1232.
[22] R. Klockenbrink, Wet Chemical Etching of Alignment V-Grooves in (100) InP through Titanium or In[sub 0.53]Ga[sub 0.47]As Masks, J. Electrochem. Soc. 141 (1994) 1594. doi:10.1149/1.2054968.
[23] S. Adachi, Chemical Etching Characteristics of (001)InP, J. Electrochem. Soc. 128 (1981) 1342. doi:10.1149/1.2127633.
[24] B.P. Minks, G. Oskam, D. Vanmaekelbergh, J.J. Kelly, Current-doubling, chemical etching and the mechanism of two-electron reduction reactions at GaAs, J. Electroanal. Chem. Interfacial Electrochem. 273 (1989) 119–131. doi:10.1016/0022-0728(89)87007-X.
[25] B.P. Minks, D. Vanmaekelbergh, J.J. Kelly, Current-doubling, chemical etching and the mechanism of two-electron reduction reactions at GaAs, J. Electroanal. Chem. Interfacial Electrochem. 273 (1989) 133–145. doi:10.1016/0022-0728(89)87008-1.
[26] A. Theuwis, I.E. Vermeir, W.P. Gomes, Chemical and electrochemical interaction of acidic H2O2 solutions with (100) InP, J. Electroanal. Chem. 410 (1996) 31–42. doi:10.1016/0022-0728(96)04532-9.
[27] H. Gerischer, W. Mindt, The mechanisms of the decomposition of semiconductors by electrochemical oxidation and reduction, Electrochimica Acta. 13 (1968) 1329–1341. doi:10.1016/0013-4686(68)80060-X.
[28] G.C. DeSalvo, W.F. Tseng, J. Comas, Etch Rates and Selectivities of Citric Acid/Hydrogen Peroxide on GaAs , Al0.3Ga0.7As , In0.2Ga0.8As , In0.53Ga0.47As , In0.52Al0.48As , and InP, J. Electrochem. Soc. 139 (1992) 831–835. doi:10.1149/1.2069311.
[29] E.M. Khoumri, A. Etcheberry, O. Poliakoff, C. Debiemme-Chouvy, J.L. Sculfort, Dissolution Rate of III–V Compound Oxides Influence of Cerium Species, J. Electrochem. Soc. 138 (1991) L65–L66.

[30] C. Debiemme-Chouvy, D. Ballutaud, J.L. Sculfort, A. Etcheberry, XPS studies of oxide layers on InP after oxidation in the presence of Ce4+, Surf. Interface Anal. 19 (1992) 393–396. doi:10.1002/sia.740190173.
[31] D.H. van Dorp, S. Arnauts, D. Cuypers, J. Rip, F. Holsteyns, S.D. Gendt, J.J. Kelly, Nanoscale Etching of In0.53Ga0.47As in H2O2/HCl Solutions for Advanced CMOS Processing, ECS J. Solid State Sci. Technol. 3 (2014) P179–P184. doi:10.1149/2.021405jss.
[32] D.H. van Dorp, S. Arnauts, F. Holsteyns, S.D. Gendt, Wet-Chemical Approaches for Atomic Layer Etching of Semiconductors: Surface Chemistry, Oxide Removal and Reoxidation of InAs (100), ECS J. Solid State Sci. Technol. 4 (2015) N5061–N5066. doi:10.1149/2.0081506jss.
[33] J. Rip, D. Cuypers, S. Arnauts, F. Holsteyns, D.H. van Dorp, S. De Gendt, Etching of III-V Materials Determined by ICP-MS with Sub-Nanometer Precision, Ecs J. Solid State Sci. Technol. 3 (2014) N3064–N3068. doi:10.1149/2.012401jss.
[34] D.Y. Petrovykh, J.M. Sullivan, L.J. Whitman, Quantification of discrete oxide and sulfur layers on sulfur-passivated InAs by XPS, Surf. Interface Anal. 37 (2005) 989–997. doi:10.1002/sia.2095.
[35] J. Meersschaut, W. Vandervorst, High-throughput ion beam analysis at imec, Nucl. Instrum. Methods Phys. Res. Sect. B Beam Interact. Mater. At. (n.d.). doi:10.1016/j.nimb.2017.01.005.
[36] M. Laitinen, M. Rossi, J. Julin, T. Sajavaara, Time-of-flight – Energy spectrometer for elemental depth profiling – Jyväskylä design, Nucl. Instrum. Methods Phys. Res. Sect. B Beam Interact. Mater. At. 337 (2014) 55–61. doi:10.1016/j.nimb.2014.07.001.
[37] J. Julin, K. Arstila, T. Sajavaara, Simulations on time-of-flight ERDA spectrometer performance, Rev. Sci. Instrum. 87 (2016) 083309. doi:10.1063/1.4961577.
[38] K. Arstila, J. Julin, M.I. Laitinen, J. Aalto, T. Konu, S. Kärkkäinen, S. Rahkonen, M. Raunio, J. Itkonen, J.-P. Santanen, T. Tuovinen, T. Sajavaara, Potku – New analysis software for heavy ion elastic recoil detection analysis, Nucl. Instrum. Methods Phys. Res. Sect. B Beam Interact. Mater. At. 331 (2014) 34–41. doi:10.1016/j.nimb.2014.02.016.
[39] D. Cuypers, S. De Gendt, S. Arnauts, K. Paulussen, D.H. van Dorp, Wet Chemical Etching of InP for Cleaning Applications: I. An Oxide Formation/Oxide Dissolution Model, ECS J. Solid State Sci. Technol. 2 (2013) P185–P189. doi:10.1149/2.020304jss.
[40] Z. Song, X-ray photoelectron spectroscopy and atomic force microscopy surface study of GaAs(100) cleaning procedures, J. Vac. Sci. Technol. B Microelectron. Nanometer Struct. 13 (1995) 77. doi:10.1116/1.587989.
[41] Shinya Osakabe and Sadao Adachi, Study of GaAs(001) Surfaces Treated in Aqueous HCl Solutions, Jpn. J. Appl. Phys. 36 (1997) 7119.
[42] Y. Ishikawa, Macroscopic electronic behavior and atomic arrangements of GaAs surfaces immersed in HCl solution, J. Vac. Sci. Technol. B Microelectron. Nanometer Struct. 12 (1994) 2713. doi:10.1116/1.587237.
[43] M.V. Lebedev, W. Calvet, T. Mayer, W. Jaegermann, Photoelectrochemical Processes at n-GaAs(100)/Aqueous HCl Electrolyte Interface: A Synchrotron Photoemission Spectroscopy Study of Emersed Electrodes, J. Phys. Chem. C. 118 (2014) 12774–12781. doi:10.1021/jp500564c.
[44] D. Cuypers, C. Fleischmann, D.H. van Dorp, S. Brizzi, M. Tallarida, M. Mueller, P. Hoenicke, A. Billen, R. Chintala, T. Conard, D. Schmeisser, W. Vandervorst, S. Van Elshocht, S. Armini, S. De Gendt, C. Adelmann, Sacrificial Self-Assembled Monolayers for the Passivation of GaAs (100) Surfaces and Interfaces, Chem. Mater. 28 (2016) 5689–5701. doi:10.1021/acs.chemmater.6b01732.
[45] M.C. Traub, J.S. Biteen, D.J. Michalak, L.J. Webb, B.S. Brunschwig, N.S. Lewis, High-Resolution X-ray Photoelectron Spectroscopy of Chlorine-Terminated GaAs(111)A Surfaces, J. Phys. Chem. B. 110 (2006) 15641–15644. doi:10.1021/jp061623n.
[46] M.C. Traub, J.S. Biteen, B.S. Brunschwig, N.S. Lewis, Passivation of GaAs Nanocrystals by Chemical Functionalization, J. Am. Chem. Soc. 130 (2008) 955–964. doi:10.1021/ja076034p.

[47] S.L. Peczonczyk, J. Mukherjee, A.I. Carim, S. Maldonado, Wet Chemical Functionalization of III–V Semiconductor Surfaces: Alkylation of Gallium Arsenide and Gallium Nitride by a Grignard Reaction Sequence, Langmuir. 28 (2012) 4672–4682. doi:10.1021/la204698a.
[48] Z.H. Lu, F. Chatenoud, M.M. Dion, M.J. Graham, H.E. Ruda, I. Koutzarov, Q. Liu, C.E.J. Mitchell, I.G. Hill, A.B. McLean, Passivation of GaAs (111) A surface by Cl termination, Appl. Phys. Lett. 67 (1995) 670–672.
[49] Y. Ishikawa, Macroscopic electronic behavior and atomic arrangements of GaAs surfaces immersed in HCl solution, J. Vac. Sci. Technol. B Microelectron. Nanometer Struct. 12 (1994) 2713. doi:10.1116/1.587237.
[50] D. Cuypers, D.H. van Dorp, M. Tallarida, S. Brizzi, T. Conard, L.N.J. Rodriguez, M. Mees, S. Arnauts, D. Schmeisser, C. Adelmann, S.D. Gendt, Study of InP Surfaces after Wet Chemical Treatments, ECS J. Solid State Sci. Technol. 3 (2014) N3016–N3022. doi:10.1149/2.005401jss.
[51] 13 - Arsenic, Antimony and Bismuth, in: Chem. Elem. Second Ed., Butterworth-Heinemann, Oxford, 1997: pp. 547–599. doi:10.1016/B978-0-7506-3365-9.50019-5.
[52] M. Pettine, L. Campanella, F.J. Millero, Arsenite oxidation by H2O2 in aqueous solutions, Geochim. Cosmochim. Acta. 63 (1999) 2727–2735. doi:10.1016/S0016-7037(99)00212-4.
[53] H. Yang, W.-Y. Lin, K. Rajeshwar, Homogeneous and heterogeneous photocatalytic reactions involving As(III) and As(V) species in aqueous media, J. Photochem. Photobiol. Chem. 123 (1999) 137–143. doi:10.1016/S1010-6030(99)00052-0.
[54] S.J. Hug, O. Leupin, Iron-Catalyzed Oxidation of Arsenic(III) by Oxygen and by Hydrogen Peroxide: pH-Dependent Formation of Oxidants in the Fenton Reaction, Environ. Sci. Technol. 37 (2003) 2734–2742. doi:10.1021/es026208x.
[55] L. Önnby, P.S. Kumar, K.G.V. Sigfridsson, O.F. Wendt, S. Carlson, H. Kirsebom, Improved arsenic(III) adsorption by Al2O3 nanoparticles and H2O2: Evidence of oxidation to arsenic(V) from X-ray absorption spectroscopy, Chemosphere. 113 (2014) 151–157. doi:10.1016/j.chemosphere.2014.04.097.
[56] D. Kim, A.D. Bokare, M. suk Koo, W. Choi, Heterogeneous Catalytic Oxidation of As(III) on Nonferrous Metal Oxides in the Presence of H2O2, Environ. Sci. Technol. 49 (2015) 3506–3513. doi:10.1021/es5056897.
[57] 12 - Phosphorus, in: Chem. Elem. Second Ed., Butterworth-Heinemann, Oxford, 1997: pp. 473–546. doi:10.1016/B978-0-7506-3365-9.50018-3.
[58] P.H.L. Notten, A. Damen, The electrochemistry of InP in Br2/HBr solutions and its relevance to etching behaviour, Appl. Surf. Sci. 28 (1987) 331–344.

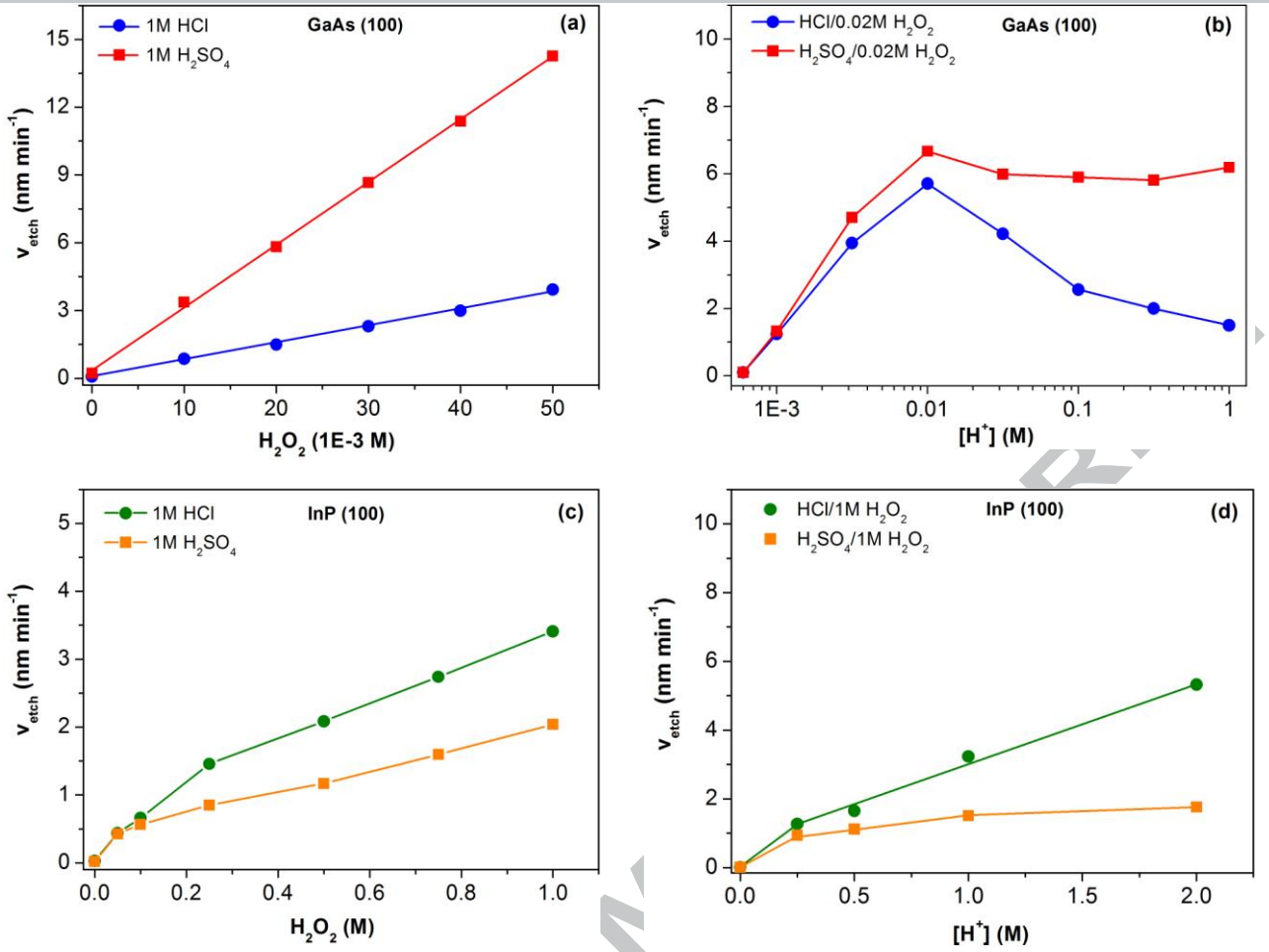

Figure 1: Etch rate of GaAs (100) as a function of H_2O_2 concentration measured by ICP-MS for 1 M HCl (circles) and 1 M H_2SO_4 solution (squares) (a). The dependence of etch rate for GaAs on the acid concentration: 0.02 M H_2O_2 in HCl and H_2SO_4 (b). Corresponding results for InP (100) are shown in (c) and (d). Note the much higher H_2O_2 concentration used in this case.

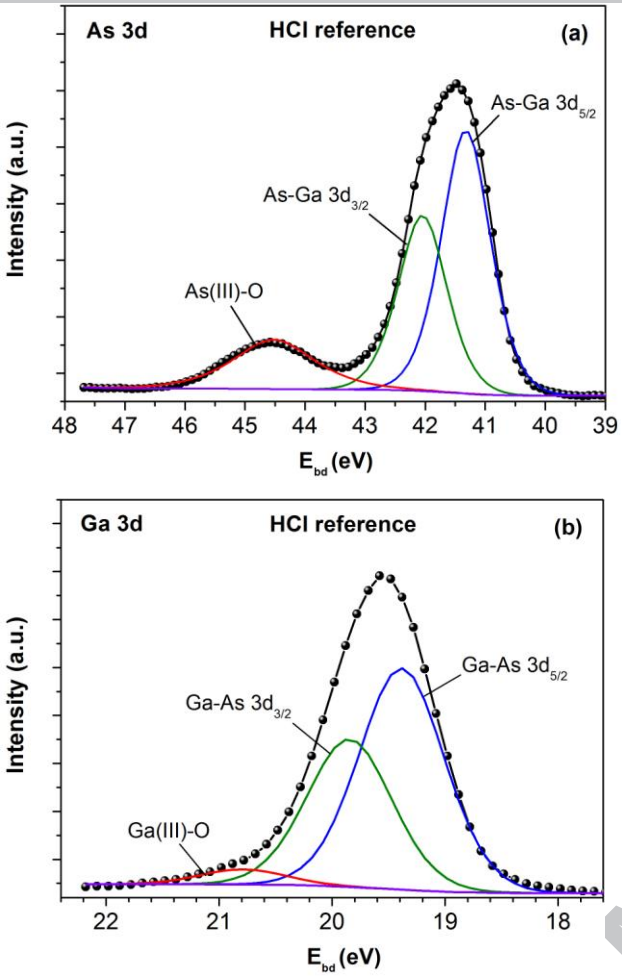

Figure 2: Angle-integrated XPS reference spectra for GaAs (100) pre-etched for 10 minutes in 6 M HCl. The As 3d and the Ga 3d peak features are shown in (a) and (b), respectively.

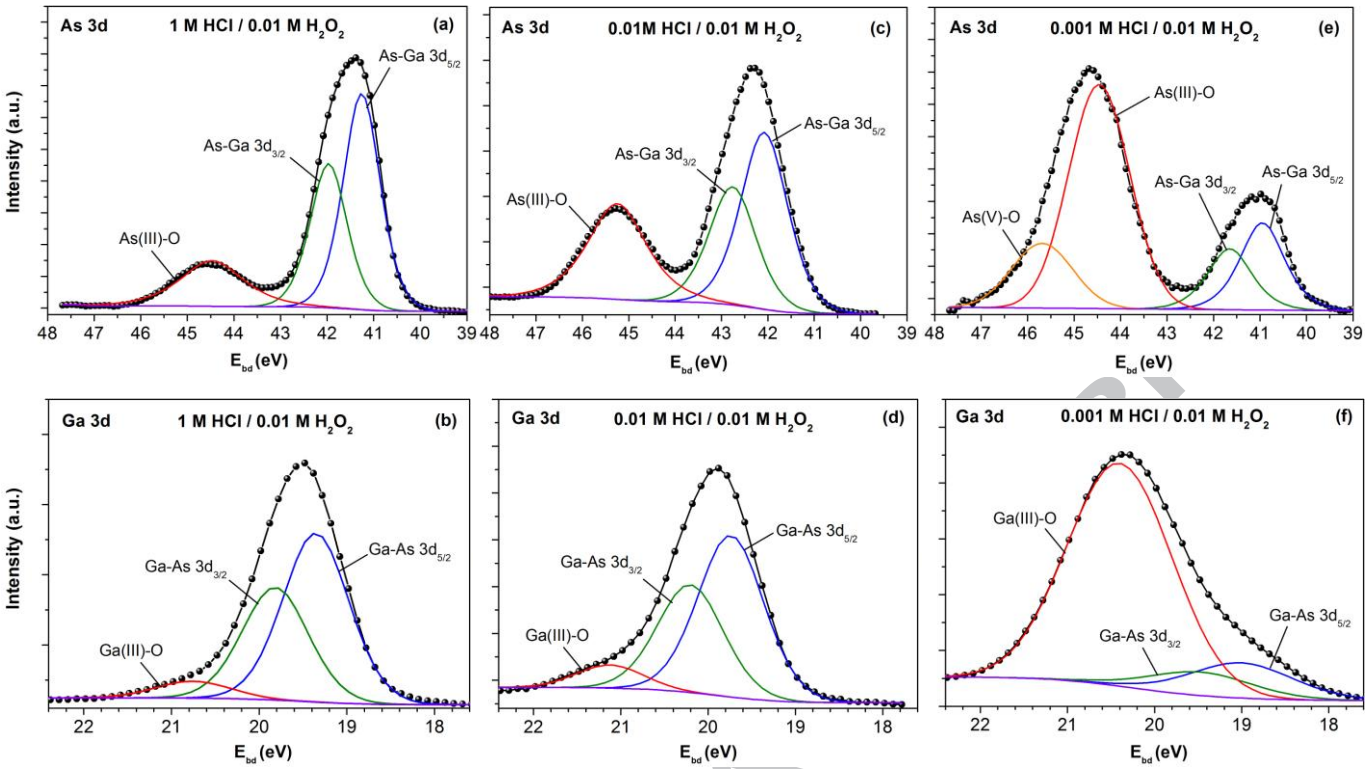

Figure 3: Angle-integrated XPS spectra showing the influence of acid concentration on the As 3d and Ga 3d peak features for GaAs (100) after 10 minutes of etching in HCl/0.01 M H_2O_2 solution: (a, b): 1 M, (c, d): 0.01 M and (e, f) 0.001 M.

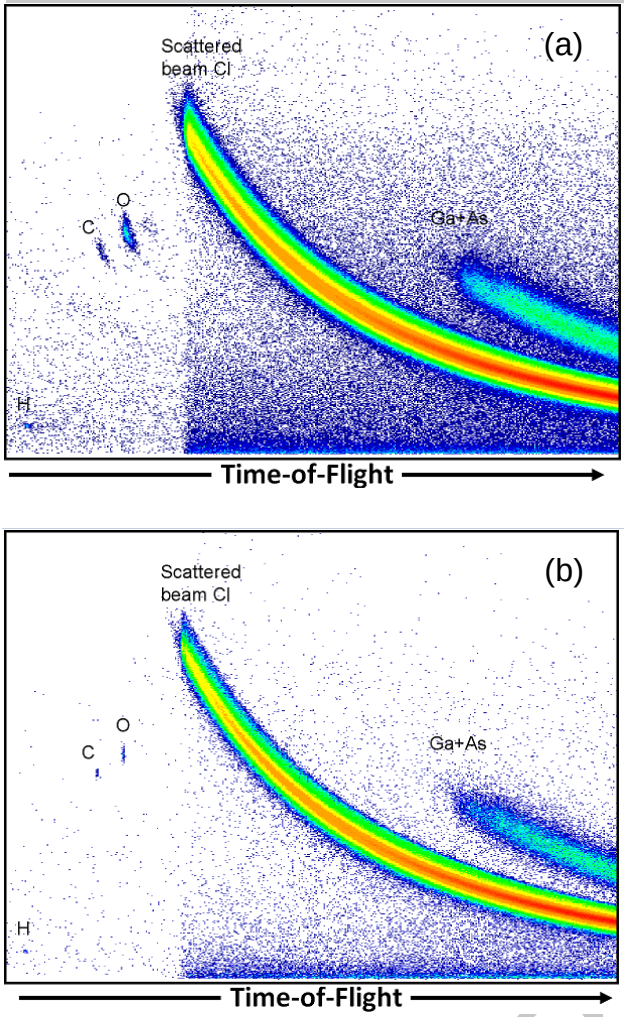

Figure 4: ToF-ERDA histograms of elemental data used for O quantification for GaAs (100) after 10 minutes of etching in 0.01 M H_2O_2 solution containing 0.001 M (a) and 0.01 M HCl (b). The sample surface is located on left of the elemental data points.

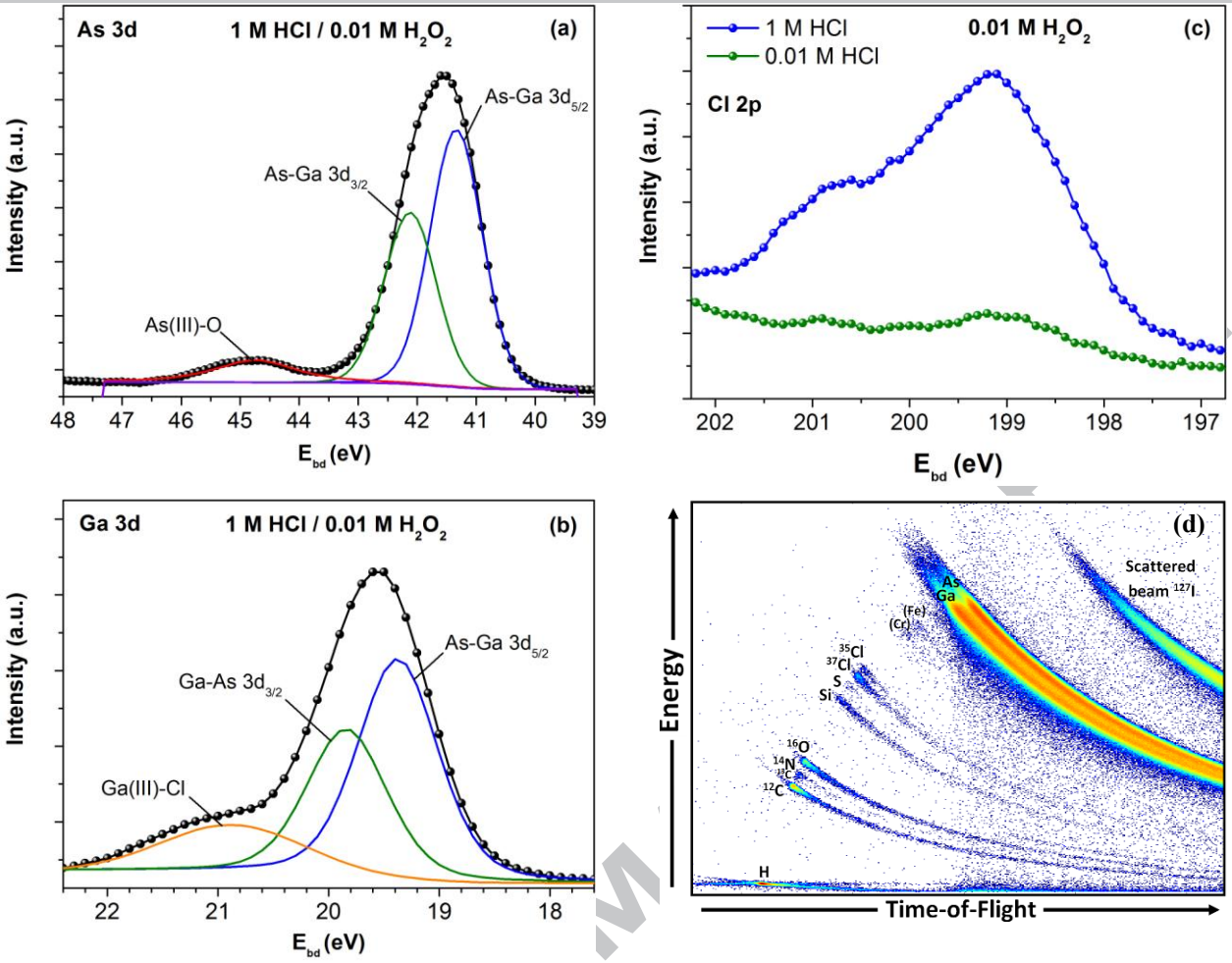

Figure 5: Angle-integrated XPS spectra showing (a) As 3d and (b) Ga 3d (b) peak features for GaAs (100) after 10 minutes of etching in HCl/0.01 M H_2O_2 solution, without UPW rinse. The corresponding Cl 2p spectrum is shown in (c) and is compared to that of a sample etched at lower HCl concentration (no UPW rinse). (d) ToF-ERDA surface elemental data used for Cl quantification for GaAs (100) after etching for 10 minutes in 1 M HCl/0.01 M H2O2 solution (d), without UPW rinse. The elongated curves for the surface elements indicate surface roughness. Note: the Cr and Fe events seen originate from sample handling.

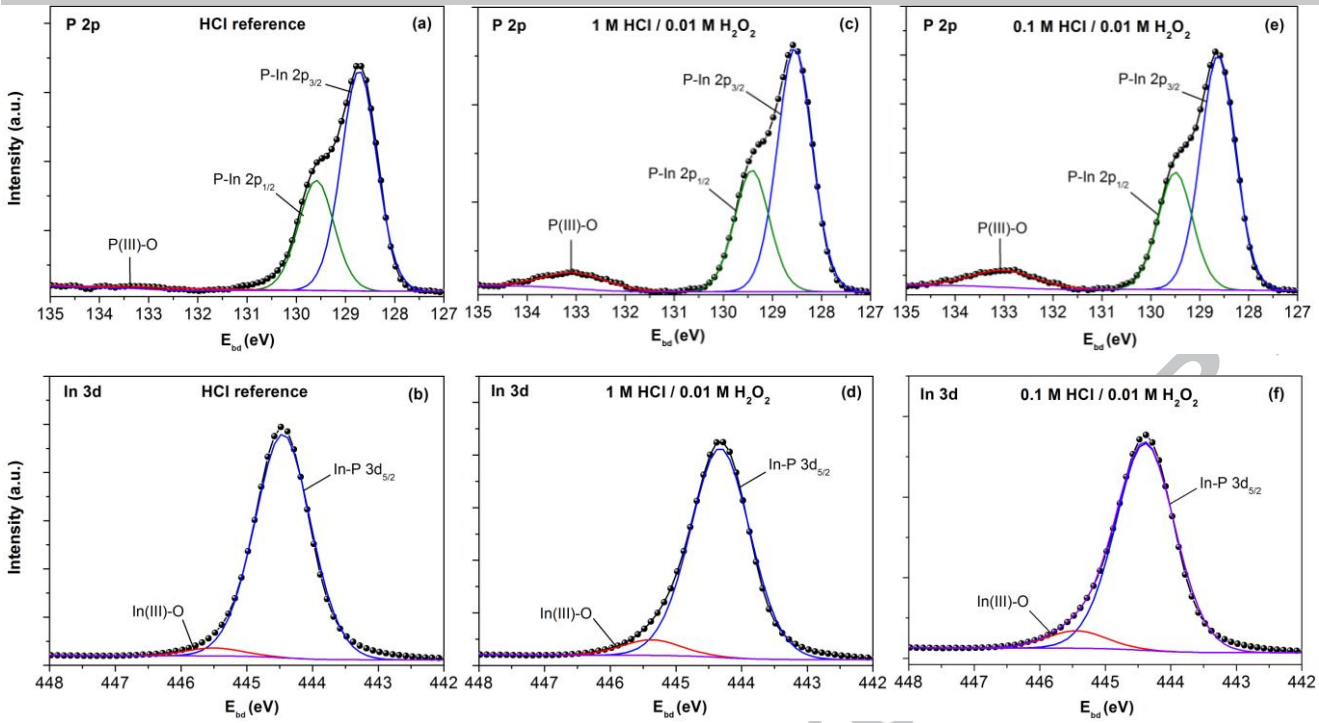

Figure 6: Angle-integrated XPS spectra for InP (100) showing P 2p and In 3d peak features for a reference sample pre-etched in 2 M HCl for 5 minutes (a, b). Spectral features for samples immersed for 10 minutes in 1 M HCl/1 M H_2O_2 and 0.1 M HCl/1 M H_2O_2 are shown in (c, d) and (e, f), respectively.

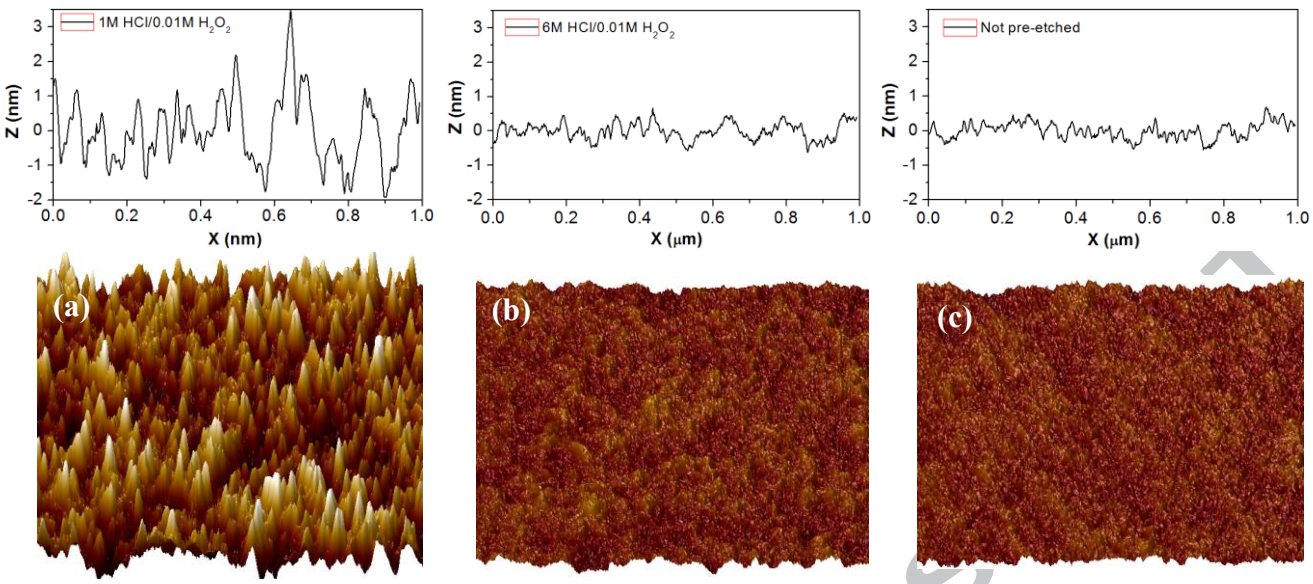

Figure 7. Tilted AFM images of GaAs surfaces: (a) after 10 nm etching in 1 M HCl/0.01 M H_2O_2 and (b) 6 M HCl/0.01 M H_2O_2. (c) shows the result for a pristine (not pre-etched) sample. In all cases, he height scale is 4 nm and the image size is 1×1 μm. The corresponding X-Z plots are shown above the AFM images.

Reaction Scheme 1: Suggested dissolution model for GaAs (100) in acidic H_2O_2 solutions (see text).

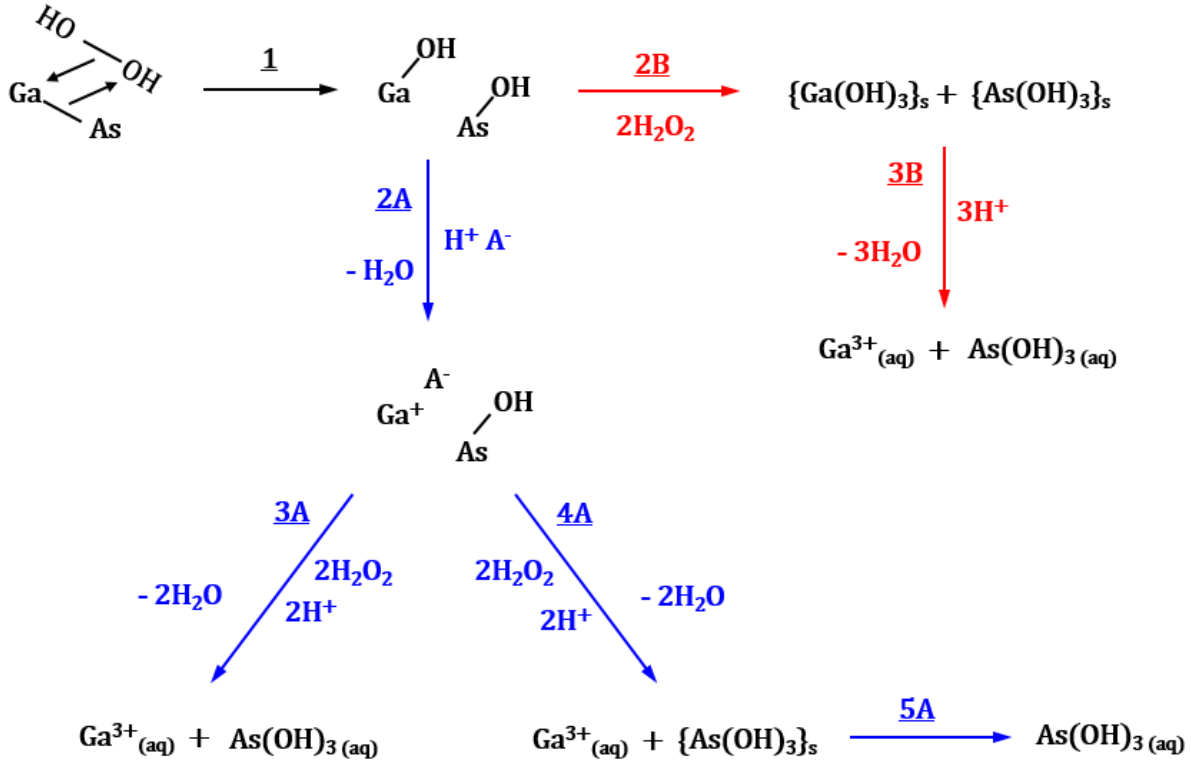

Reaction Scheme 2: Suggested dissolution model for InP (100) in acidic H_2O_2 solutions (see text).

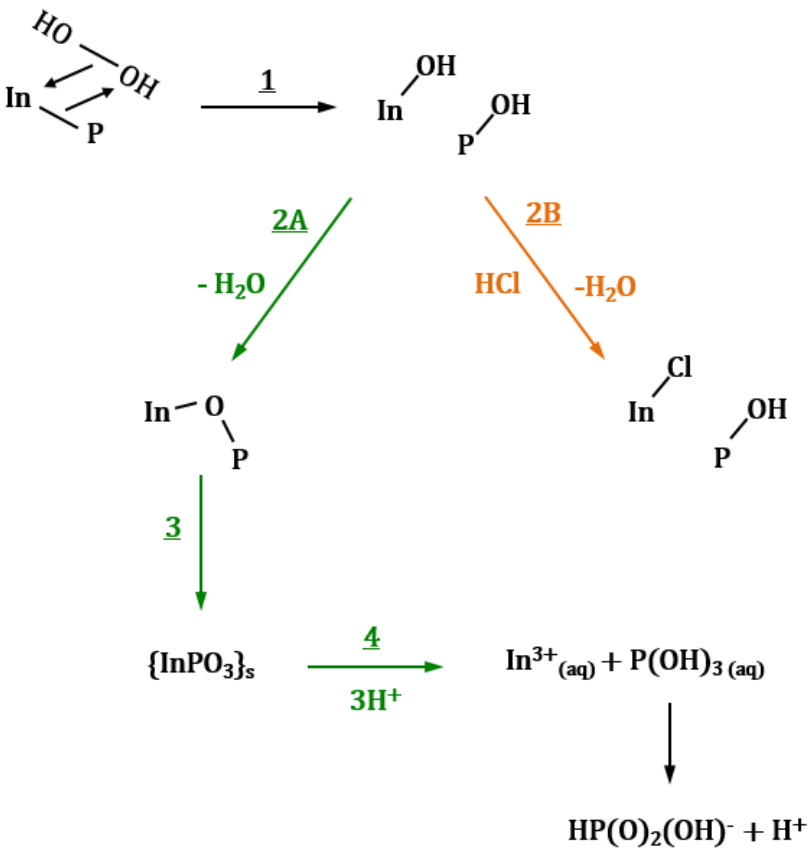

Reaction Scheme 3: Proposed model for oxygen bridge formation during the dissolution of InP in acidic H_2O_2 solutions (see text).

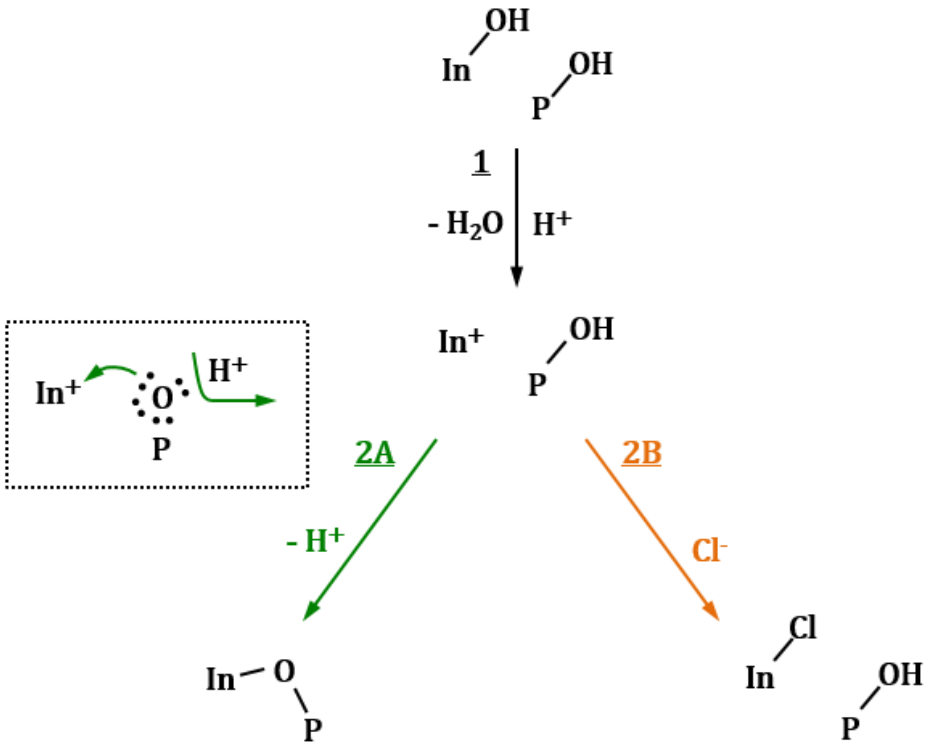

The critical step in oxide formation

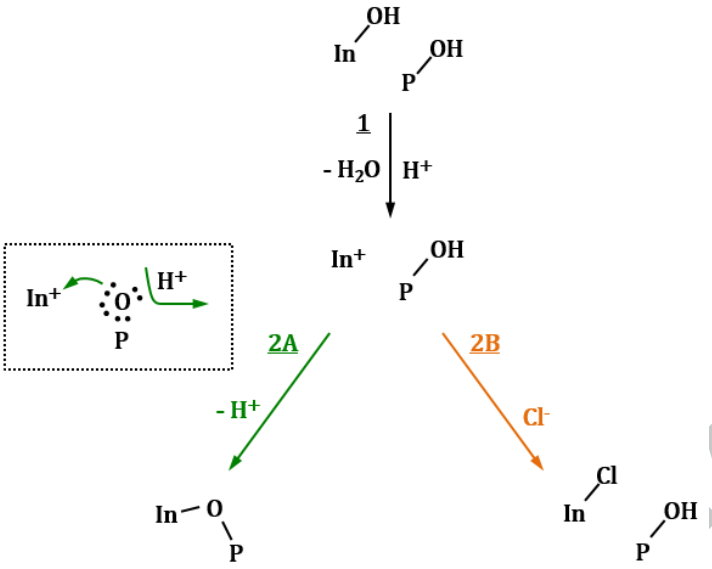

Highlights

Two different etching regimes are observed for GaAs

With striking differences in surface oxide

Strong influence of Cl- on etch rate and surface roughness (of GaAs)

Lower chemical reactivity of InP due to In-O-P bridge formation

Surface acidity can explain marked differences in results for GaAs and InP